

Magnetic Response in a Zigzag Carbon Nanotube

Paramita Dutta,¹ Santanu K. Maiti,^{2,*} and S. N. Karmakar¹

¹*Theoretical Condensed Matter Physics Division, Saha Institute of Nuclear Physics,
Sector-I, Block-AF, Bidhannagar, Kolkata-700 064, India*

²*School of Chemistry, Tel Aviv University, Ramat-Aviv, Tel Aviv-69978, Israel*

Magnetic response of interacting electrons in a zigzag carbon nanotube threaded by a magnetic flux is investigated within a Hartree-Fock mean field approach. Following the description of energy spectra for both non-interacting and interacting cases we analyze the behavior of persistent current in individual branches of a nanotube. Our present investigation leads to a possibility of getting a filling-dependent metal-insulator transition in a zigzag carbon nanotube.

PACS numbers: 73.23.-b, 73.23.Ra.

I. INTRODUCTION

The isolation of single layer graphene by Novoselov *et al.* [1] has initiated intense and diverse research on this system. Graphene, a single layer of carbon atoms tightly packed into a two-dimensional honey-comb lattice, has drawn attention of scientists in various disciplines due to its unconventional and fascinating electronic properties arising particularly from the linear dispersion relation around the Dirac points of the hexagonal Brillouin zone. These unique properties can be understood in terms of the Dirac Hamiltonian [2] since it actually describes the physics of electrons near the Fermi level of the undoped material. The carriers in graphene effectively behave as massless relativistic particles within a low energy range close to Fermi energy and these massless Dirac Fermions [3] evince various phenomena in this energy range. The bipartite character of the wonderful lattice structure of graphene strongly influences its intrinsic properties and makes graphene a wonderful testbed not only for condensed matter theory, but also for quantum field theory and mathematical physics. Though lot of studies have been done both theoretically as well as experimentally to reveal electronic properties of this exotic system, yet complete knowledge about it is still lacking. This motivates us to address some interesting issues of electron transport in carbon nanotubes where a nanotube is formed by rolling up a graphite ribbon in the cylindrical form [4].

In this article we explore the behavior of persistent current in a finite sized graphite nanotube with zigzag edges within a nearest-neighbor tight-binding (TB) framework using a generalized Hartree-Fock (HF) approximation [5–7]. The phenomenon of persistent current in a mesoscopic ring, threaded by an Aharonov-Bohm (AB) flux ϕ , has been studied theoretically more than two decades ago [8–11]. Later it has been justified through several nice experiments [12–15]. It is a pure quantum mechanical effect and can persist without any dissipation in the equilib-

rium case. In the last few years extensive studies on persistent current in carbon nanotubes have been performed and many interesting physical phenomena have been explored [16–18]. Persistent current in a carbon nanotube is highly sensitive to its radius, chirality, deformation, etc. Very recently it has also been observed experimentally that the Fermi energy of a carbon nanotube can be regulated nicely by means of electron or hole doping, which can induce a dramatic change in persistent current [18]. It is well established that in a conventional multi-channel mesoscopic cylinder electron transport strongly depends on the correlation among different channels as well as the shape of Fermi surface. Therefore we might expect some

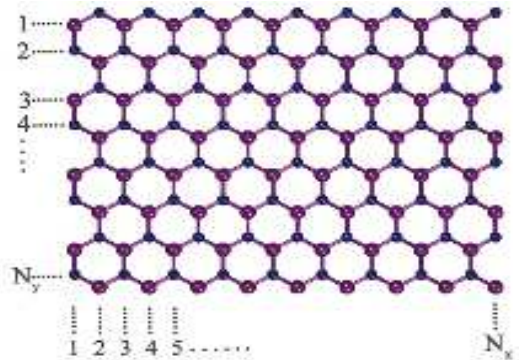


FIG. 1: (Color online). Schematic view of a zigzag graphite nano-ribbon with N_x and N_y number of atomic sites along the x and y directions, respectively.

interesting features of persistent current in a carbon nanotube due to its unique electronic structure.

The behavior of persistent current in zigzag nanotubes has been addressed theoretically by some groups [16–18]. There are many theoretical techniques available in the literature [19–24] which generally investigate magnetic response of the entire system but the distribution of persistent current among different branches of the nanotube remains unaddressed though it is highly important to illuminate the magnetic response of the system with a deeper insight. To the best of our knowledge, no rigorous effort has been made so far to unravel the behavior

*Electronic address: santanu@post.tau.ac.il

of persistent current in separate branches of a graphite nanotube. This is the main motivation behind this work.

In what follows, we present the results. Section II is devoted to present the model and generalized HF approach. Following the energy spectra for the non-interacting and interacting cases (Section III), in Section IV we establish the second quantized form to evaluate persistent current in individual branches of a zigzag carbon nanotube. The energy-flux characteristics are described in Section V, while the behavior of persistent current in separate branches of a nanotube is illustrated in Section VI. Finally, in Section VII we draw our conclusions.

II. THE MODEL AND THE MEAN FIELD APPROACH

We begin with a graphite nano-ribbon of zigzag edges as shown in Fig. 1, where the filled magenta (large) and blue (small) circles correspond to two different sublattices, namely, A and B, respectively. N_x and N_y correspond to the number of atomic sites along the x and

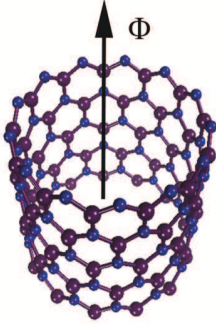


FIG. 2: (Color online). A graphite nanotube threaded by a magnetic flux Φ .

y directions, respectively. In order to elucidate magnetic response of a nanotube we roll up the graphite ribbon along x direction using periodic boundary condition and allow to pass a magnetic flux ϕ (measured in unit of elementary flux quantum $\phi_0 = ch/e$) along the axis of the tube as shown in Fig. 2. We describe our model quantum system by the nearest-neighbor TB framework which captures most of the essential properties of the tube nicely [25–28]. In presence of magnetic flux ϕ , the Hamiltonian of an interacting zigzag nanotube reads,

$$\begin{aligned}
 H = & t \sum_{m,n,\sigma} (a_{m,n,\sigma}^\dagger b_{m-1,n,\sigma} e^{-i\theta} + a_{m,n,\sigma}^\dagger b_{m+1,n,\sigma} e^{i\theta} \\
 & + a_{m,n,\sigma}^\dagger b_{m,n+1,\sigma}) + \text{h.c.} \\
 & + U \sum_{m,n} (a_{m,n,\uparrow}^\dagger a_{m,n,\uparrow} a_{m,n,\downarrow}^\dagger a_{m,n,\downarrow} \\
 & + b_{m+1,n,\uparrow}^\dagger b_{m+1,n,\uparrow} b_{m+1,n,\downarrow}^\dagger b_{m+1,n,\downarrow}) \quad (1)
 \end{aligned}$$

where, m and n are integers describing the co-ordinates of the lattice sites. The site indexing is schematically shown in Fig. 3 for better viewing. t is the nearest-neighbor hopping integral, $a_{m,n}^\dagger$ ($b_{m,n}^\dagger$) is the creation operator for an electron of spin σ (\uparrow, \downarrow) associated with A (B) type of sites at the position (m,n) and the corresponding anni-

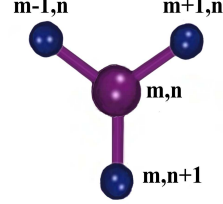


FIG. 3: (Color online). Schematic view of different atomic sites with their co-ordinates.

hilation operator is denoted by $a_{m,n}$ ($b_{m,n}$). The factor θ ($= 2\pi\phi/N_x$), the so-called Peierl's phase factor, is introduced into the above Hamiltonian to incorporate the effect of magnetic flux applied along the axis of the tube. U is the strength of on-site Hubbard interaction.

Decoupling of interacting Hamiltonian. Using the generalized HF approach, we decouple the TB Hamiltonian into two different parts corresponding to two different values of σ (\uparrow and \downarrow). After decoupling, the Hamiltonian looks like,

$$H_{\text{MF}} = H_\uparrow + H_\downarrow + H_0 \quad (2)$$

where,

$$\begin{aligned}
 H_\uparrow = & U \sum_{m,n} (\langle n_{m,n,\downarrow}^a \rangle n_{m,n,\uparrow}^a + \langle n_{m+1,n,\downarrow}^b \rangle n_{m+1,n,\uparrow}^b) \\
 & + t \sum_{m,n} (a_{m,n,\uparrow}^\dagger b_{m-1,n,\uparrow} e^{-i\theta} + a_{m,n,\uparrow}^\dagger b_{m+1,n,\uparrow} e^{i\theta} \\
 & + a_{m,n,\uparrow}^\dagger b_{m,n+1,\uparrow} + \text{h.c.}), \quad (3)
 \end{aligned}$$

$$\begin{aligned}
 H_\downarrow = & U \sum_{m,n} (\langle n_{m,n,\uparrow}^a \rangle n_{m,n,\downarrow}^a + \langle n_{m+1,n,\uparrow}^b \rangle n_{m+1,n,\downarrow}^b) \\
 & + t \sum_{m,n} (a_{m,n,\downarrow}^\dagger b_{m-1,n,\downarrow} e^{-i\theta} + a_{m,n,\downarrow}^\dagger b_{m+1,n,\downarrow} e^{i\theta} \\
 & + a_{m,n,\downarrow}^\dagger b_{m,n+1,\downarrow} + \text{h.c.}) \quad (4)
 \end{aligned}$$

and

$$\begin{aligned}
 H_0 = & -U \sum_{m,n} (\langle n_{m,n,\uparrow}^a \rangle \langle n_{m,n,\downarrow}^a \rangle \\
 & + \langle n_{m+1,n,\uparrow}^b \rangle \langle n_{m+1,n,\downarrow}^b \rangle). \quad (5)
 \end{aligned}$$

Here, $n_{m,n,\sigma}^a$ and $n_{m,n,\sigma}^b$ are the number operators associated with the A and B types of atoms, respectively. H_\uparrow and H_\downarrow are the Hamiltonians for up and down spin

electrons, respectively. H_0 is a constant term which gives the energy shift.

Self-consistent procedure: In order to get the energy eigenvalues of the interacting Hamiltonian we go through a self-consistent procedure considering initial guess values of $\langle n_{m,n,\sigma}^a \rangle$ and $\langle n_{m,n,\sigma}^b \rangle$. With these initial values, the up and down spin Hamiltonians are diagonalized numerically and a new set of values of $\langle n_{m,n,\sigma}^a \rangle$ and $\langle n_{m,n,\sigma}^b \rangle$ are calculated. These steps are repeated until a self-consistent solution is achieved.

Finding the ground state energy: After getting the self-consistent solution we determine the ground state energy (E_0) at absolute zero temperature ($T = 0 K$) for a particular filling by taking the sum of individual states upto the Fermi level (E_F) for both up and down spin electrons. The expression for ground state energy reads,

$$E_0 = \sum_i E_{i,\uparrow} + \sum_i E_{i,\downarrow} + H_0 \quad (6)$$

where, i runs over the states up to the Fermi level. $E_{i,\uparrow}$'s and $E_{i,\downarrow}$'s are the single particle energy eigenvalues obtained by diagonalizing the up and down spin Hamiltonians H_\uparrow and H_\downarrow , respectively.

III. ENERGY SPECTRUM

To make this present communication a self contained study let us first start with the energy band structure of a finite width zigzag nano-ribbon.

Non-interacting case: To establish the energy dispersion relation of a zigzag nano-ribbon we find an effective dif-

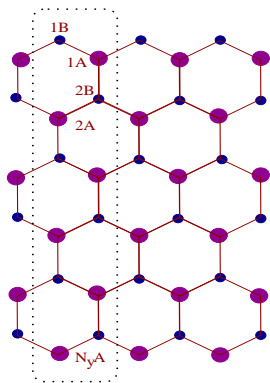


FIG. 4: (Color online). Unit cell configuration of a zigzag nano-ribbon.

ference equation analogous to the case of an infinite one-dimensional chain. This can be done by proper choice of a unit cell from the nano-ribbon. The schematic view of a unit cell configuration with N_y pairs of B-A atoms in a zigzag nano-ribbon is shown in Fig. 4. With this arrangement, the effective difference equation of the nano-ribbon

gets the form,

$$(E\mathcal{I} - \mathcal{E}_\sigma)\psi_{j,\sigma} = \mathcal{T}\psi_{j+1,\sigma} + \mathcal{T}^\dagger\psi_{j-1,\sigma} \quad (7)$$

where,

$$\psi_{j,\sigma} = \begin{pmatrix} \psi_{j1B,\sigma} \\ \psi_{j1A,\sigma} \\ \psi_{j2B,\sigma} \\ \vdots \\ \psi_{jN_yA,\sigma} \end{pmatrix}. \quad (8)$$

\mathcal{E} and \mathcal{T} are the site-energy and nearest-neighbor hopping matrices of the unit cell, respectively. \mathcal{I} is a $(2N_y \times 2N_y)$ identity matrix. Since in the nano-ribbon translational invariance exists along the x -direction, we can write $\psi_{j,\sigma}$ in terms of the Bloch waves and then Eq. 7 takes the form,

$$(E\mathcal{I} - \mathcal{E}_\sigma) = \mathcal{T}e^{ik_x\Lambda} + \mathcal{T}^\dagger e^{-ik_x\Lambda} \quad (9)$$

where, $\Lambda = \sqrt{3}a$ is the horizontal separation between two filled magenta or blue circles situated at two successive unit cells. a is the length of each side of a hexagonal benzene like ring. Solving Eq. 9 we get the desired energy dispersion relation (E vs. k_x) of the ribbon.

As illustrative example, in Fig. 5 we show the variation of energy levels (green curves) as a function of wave vector k_x for a finite width zigzag nano-ribbon considering

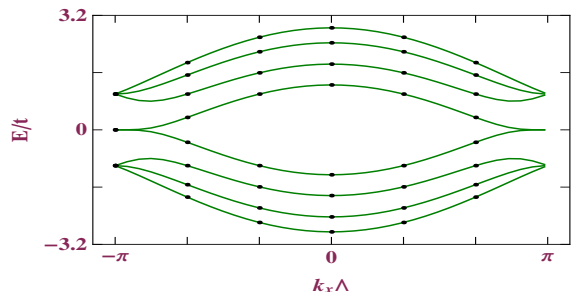


FIG. 5: (Color online). Energy levels (green curve) as function of k_x for a finite width zigzag nano-ribbon considering $N_y = 4$. The discrete eigenvalues (filled black circles) of a nanotube with $N_x = 12$ and $N_y = 4$, in the absence of AB flux ϕ , are superimposed. Here we set $U = 0$.

$N_y = 4$. Quite interestingly we observe that at $E = 0$, partly flat bands appear in the spectrum which make the system unique. The electronic states corresponding to those almost flat bands are characterized by strongly localized states near the zigzag edges of the tube. The existence of these edge states have also been reported earlier by some other groups [2, 29, 30].

Following the energy band structure of a finite width nano-ribbon now we focus on the variation of energy levels of a nanotube. For a nanotube k_x also becomes quantized where the quantized values are obtained

by applying periodic boundary condition along the x -direction [31]. The quantized wave numbers are expressed from the relation $k_x = 4\pi n_x/N_x\Lambda$, where n_x is an integer lies within the range: $-N_x/4 \leq n_x < N_x/4$. Plugging the quantized values of k_x in Eq. 9 we can easily determine the eigenvalues of a finite sized nanotube. As representative example, in Fig. 5 we show the variation of discrete energy eigenvalues (filled black circles) for a zigzag nanotube considering $N_x = 12$ and $N_y = 4$, in the absence of AB flux ϕ passing through the tube. For this nanotube k_x gets six quantized values ($-\pi/\Lambda, -2\pi/3\Lambda, -\pi/3\Lambda, 0, \pi/3\Lambda$ and $2\pi/3\Lambda$), and therefore, total 48 energy values are obtained since N_y is set at 4.

Interacting case: In the presence of e-e interaction energy levels get modified significantly depending on the filling of electrons. The results calculated for a particular value

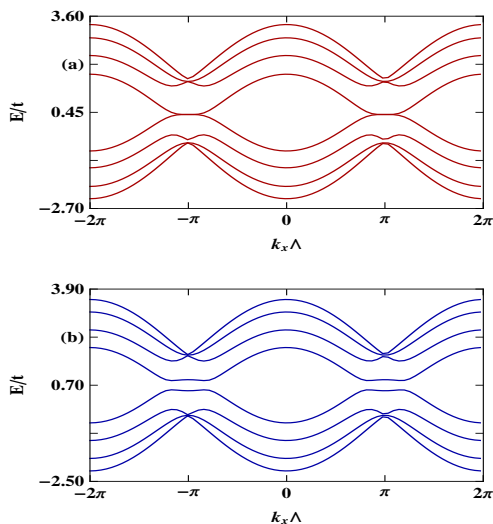


FIG. 6: (Color online). Energy levels as function of k_x for a finite width zigzag nano-ribbon considering $N_y = 4$ and $U = 1.4$, where (a) and (b) correspond to the one-third- and half-filled cases, respectively.

of U are presented in Fig. 6 where we set $N_y = 4$. In the half-filled band case, a gap opens up at the Fermi energy [32] which is consistent with the DFT calculations [33] and the gap increases with the value of U . A careful investigation also predicts that the full energy band gets shifted by the factor $U/2$.

IV. SECOND QUANTIZED FORM OF PERSISTENT CURRENT

In order to evaluate persistent current in individual zigzag paths of a nanotube, threaded by an AB flux ϕ , we use second quantized approach [34, 35]. This is an elegant and nice way of studying the response in separate branches of any quantum network.

We start with the basic equation of current operator \mathbf{I}_σ corresponding to spin σ in terms of the velocity operator

$\mathbf{v}_\sigma (= \dot{\mathbf{x}}_\sigma)$ as,

$$\mathbf{I}_\sigma = -\frac{1}{N_x} e \dot{\mathbf{x}}_\sigma \quad (10)$$

where, \mathbf{x}_σ is the displacement operator. The velocity operator is computed from the expression,

$$\mathbf{v}_\sigma = \frac{1}{i\hbar} [\mathbf{x}_\sigma, \mathbf{H}_\sigma]. \quad (11)$$

Using this relation we can write the velocity operator of an electron with spin σ in a zigzag channel n (say) in the

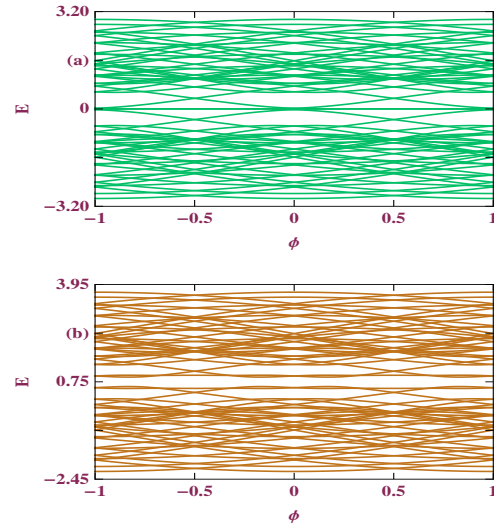


FIG. 7: (Color online). Energy-flux characteristics of a half-filled zigzag nanotube with $N_x = 10$ and $N_y = 7$. (a) $U = 0$ and (b) $U = 1.5$.

form,

$$\begin{aligned} \mathbf{v}_{n,\sigma} = & \frac{t}{i\hbar} \sum_m \left(b_{m+1,n,\sigma}^\dagger a_{m,n,\sigma} e^{-i\theta} \right. \\ & - a_{m,n,\sigma}^\dagger b_{m+1,n,\sigma} e^{i\theta} - b_{m-1,n,\sigma}^\dagger a_{m,n,\sigma} e^{i\theta} \\ & \left. + a_{m,n,\sigma}^\dagger b_{m-1,n,\sigma} e^{-i\theta} \right). \end{aligned} \quad (12)$$

Therefore, for a particular eigenstate $|\psi_{p,\sigma}\rangle$ persistent current in n -th channel becomes,

$$I_{n,\sigma}^p = -\frac{e}{N_x} \langle \psi_{p,\sigma} | \mathbf{v}_{n,\sigma} | \psi_{p,\sigma} \rangle \quad (13)$$

where, the eigenstate $|\psi_{p,\sigma}\rangle$ looks like,

$$\begin{aligned} |\psi_{p,\sigma}\rangle = & \sum_{m,n} \left(\alpha_{m,n,\sigma}^p |m, n, \sigma\rangle + \beta_{m-1,n,\sigma}^p |m-1, n, \sigma\rangle \right. \\ & + \beta_{m+1,n,\sigma}^p |m+1, n, \sigma\rangle \\ & \left. + \beta_{m,n+1,\sigma}^p |m, n+1, \sigma\rangle \right). \end{aligned} \quad (14)$$

Here, $|m, n, \sigma\rangle$'s are the Wannier states and $\alpha_{m,n,\sigma}^p$ and $\beta_{m,n,\sigma}^p$'s are the corresponding coefficients. Simplifying

Eq. 13, we get the final relation of persistent charge current for n -th zigzag channel as,

$$I_{n,\sigma}^p = \frac{iet}{\hbar N_x} \sum_m (\beta_{m+1,n,\sigma}^{p*} \alpha_{m,n,\sigma}^p e^{-i\theta} - \alpha_{m,n,\sigma}^{p*} \beta_{m+1,n,\sigma}^p e^{i\theta} - \beta_{m-1,n,\sigma}^{p*} \alpha_{m,n,\sigma}^p e^{i\theta} + \alpha_{m,n,\sigma}^{p*} \beta_{m-1,n,\sigma}^p e^{-i\theta}). \quad (15)$$

$$I_{m-1,m,\sigma}^p = \frac{it}{2\hbar N_y} \left[\sum_{n=1,3,\dots}^{N_y} (\alpha_{m,n,\sigma}^{p*} \beta_{m-1,n,\sigma}^p e^{-i\theta} - \beta_{m-1,n,\sigma}^{p*} \alpha_{m,n,\sigma}^p e^{i\theta}) + \sum_{n=2,4,\dots}^{N_y} (\beta_{m,n,\sigma}^{p*} \alpha_{m-1,n,\sigma}^p e^{-i\theta} - \alpha_{m-1,n,\sigma}^{p*} \beta_{m,n,\sigma}^p e^{i\theta}) \right. \\ \left. \times \beta_{m,n,\sigma}^p e^{i\theta} + \beta_{m-1,n,\sigma}^{p*} \alpha_{m-1,n-1,\sigma}^p - \alpha_{m-1,n-1,\sigma}^{p*} \beta_{m-1,n,\sigma}^p \right] + \sum_{n=2,4,\dots}^{N_y-1} (\beta_{m,n+1,\sigma}^{p*} \alpha_{m,n,\sigma}^p - \alpha_{m,n,\sigma}^{p*} \beta_{m,n+1,\sigma}^p) \quad (16)$$

where, an armchair channel $(m-1, m)$ is constructed by $(m-1)$ -th and m -th lines according to our indexing.

At absolute zero temperature ($T = 0 K$), net persistent current driven by electrons of spin σ in a particular

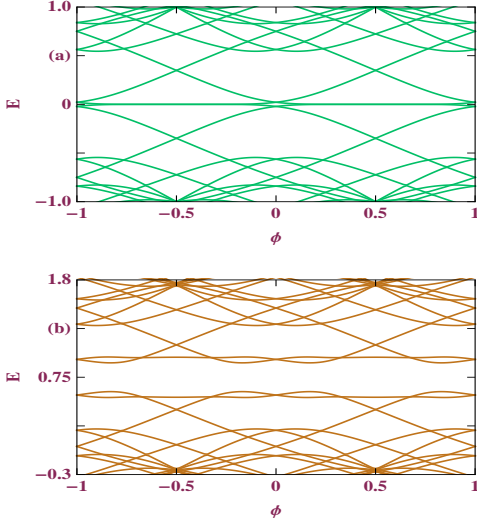


FIG. 8: (Color online). Few energy levels of Fig. 7 are replotted for a narrow energy range across the band centres for better viewing of the variation of energy levels with flux ϕ , where (a) and (b) correspond to the identical meaning as in Fig. 7.

channel n for a nanotube described with Fermi energy E_F can be determined by taking the sum of individual contributions from the lowest energy eigenstates upto the Fermi level. Hence we get,

$$I_{n,\sigma} = \sum_p I_{n,\sigma}^p. \quad (17)$$

Using the same prescription we can also evaluate persistent current in individual armchair paths (along y direction) of the nanotube. The final expression of it gets the form,

Summing $I_{n,\sigma}$ over all possible channels n , and σ we get total persistent current in the nanotube which is mathematically expressed as,

$$I_T = \sum_{n,\sigma} I_{n,\sigma}. \quad (18)$$

The persistent current can also be determined in some other ways as available in literature. Probably the sim-

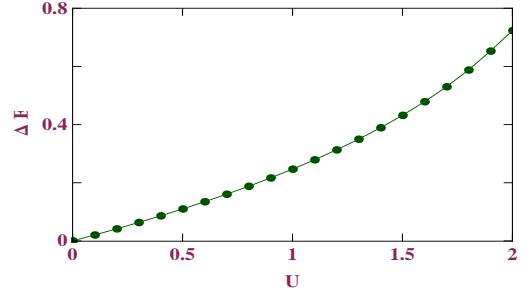


FIG. 9: (Color online). Energy gap (ΔE) as a function of on-site Hubbard interaction strength U for a zigzag nanotube with $N_x = 10$ and $N_y = 7$ in the half-filled band case when ϕ is set at $\phi_0/2$.

plest way of determining persistent current is the case where first order derivative of ground state energy with respect to AB flux ϕ is taken into account. Therefore, we can write,

$$I_T = -c \frac{\partial E_0(\phi)}{\partial \phi} \quad (19)$$

where, $E_0(\phi)$ is the total ground state energy for a particular electron filling. But, in our present scheme, the so-called second quantized approach, there are some advantages compared to other available procedures. Firstly,

we can easily measure current in any branch of a complicated network. Secondly, the determination of individual responses in separate branches helps us to elucidate the actual mechanism of electron transport in a more transparent way.

In the present work we examine all the essential features of persistent current at absolute zero temperature and use the units where $c = h = e = 1$. Throughout our numerical calculations we set $t = -1$ and measure all the physical quantities in unit of t .

V. ENERGY-FLUX CHARACTERISTICS

In Fig. 7 we show the variation of energy levels as a function of flux ϕ for a zigzag nanotube considering $N_x = 10$ and $N_y = 7$ both for the (a) non-interacting

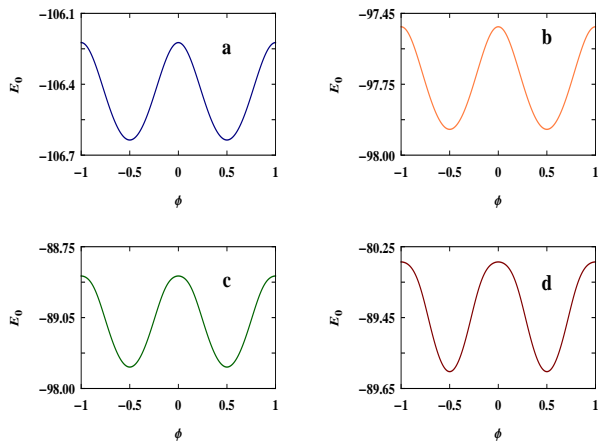


FIG. 10: (Color online). Ground state energy level as a function of ϕ for a zigzag nanotube in the half-filled band case considering $N_x = 20$ and $N_y = 8$. (a), (b), (c) and (d) correspond to $U = 0, 0.5, 1$ and 1.5 , respectively.

and (b) interacting cases. For $U = 0$, we compute the energy levels simply by diagonalizing the non-interacting Hamiltonian and the nature of the energy spectrum becomes independent of the total number of electrons N_e in the system. On the other hand, for the non-interacting case ($U \neq 0$) we first decouple the interacting Hamiltonian (Eq. 1) for a particular filling, in the mean field scheme, into two non-interacting Hamiltonians (for up and down spin electrons) and then diagonalize the Hamiltonian for up (down) spin electrons. For identical filling factor of up and down spin electrons the energy levels are exactly similar both for H_\uparrow and H_\downarrow (see Fig. 7(b)), and therefore, one energy spectrum cannot be separated from the other. Since in our case we set $N_x = 10$ and $N_y = 7$, we get total 70 independent energy levels and due to their overlaps individual energy levels are not clearly distinguished from the spectra given in Fig. 7. To have a better look in Fig. 8 we re-plot few energy levels of Fig. 7 collecting them from a narrow energy range across the

band centres, where (a) and (b) correspond to the identical meaning as in Fig. 7. From the spectra we see that all the energy levels vary periodically with ϕ providing $\phi_0 (= 1$ in our chosen unit) flux-quantum periodicity. At half-integer or integer multiples of ϕ_0 , energy levels have either a maximum or a minimum (see Fig. 8), and accordingly, at these points persistent current becomes zero which is quite obvious since the current is obtained by taking the first order derivative of the eigenenergy with respect to flux ϕ (Eq. 19). Both the energy spectra take a complicated look as there are many crossings among the energy levels particularly in the regions away from $E = 0$ (Fig. 8). At $E = 0$, the energy levels become almost flat for a wide range of ϕ , and, near $\phi = \pm\phi_0/2$ they vary slowly with ϕ as shown in Fig. 8(a). These almost flat energy levels support a very little contribution

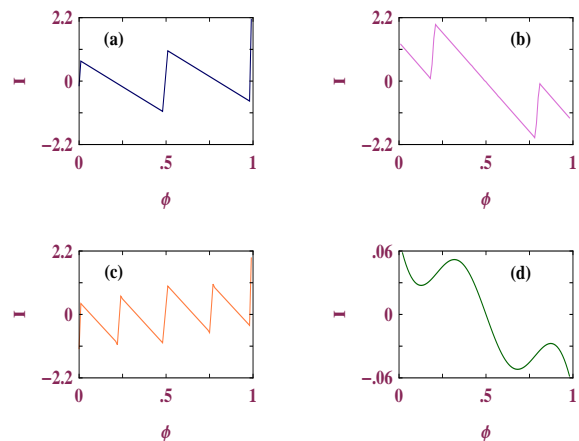


FIG. 11: (Color online). Current-flux characteristics of a zigzag nanotube with $N_x = 14$ and $N_y = 6$, where (a), (b), (c) and (d) correspond to $N_e = 10, 20, 30$ and 82 , respectively. U is fixed at 1.

to the persistent current as clearly followed from Eq. 19. While, the other energy levels with larger slopes provide large persistent current. This peculiar nature of the energy levels invokes the *current amplitude to become filling dependent* and we elaborate it in the following section. In Fig. 7(b) we display the variation of energy levels with ϕ for a zigzag nanotube with the same parameter values declared above in the presence of Hubbard interaction. Here we choose $U = 1.5$. Both for the up and down spin Hamiltonians the eigenvalues are exactly identical and they overlap with each other. Few energy levels of Fig. 7(b) are also re-plotted in Fig. 8(b) for better viewing. The electronic correlation leads to an energy gap at the band centre and the gap increases with U . It is illustrated in Fig. 9. This energy gap is consistent with the energy gap obtained in the $E-k_x$ diagram (Fig. 6(b)).

The variation of ground state energy level of a carbon nanotube with zigzag edges as a function of magnetic flux ϕ is depicted in Fig. 10 in the half-filled band case, where (a), (b), (c) and (d) correspond to the four different values of electronic correlation strength $U = 0, 0.5, 1$

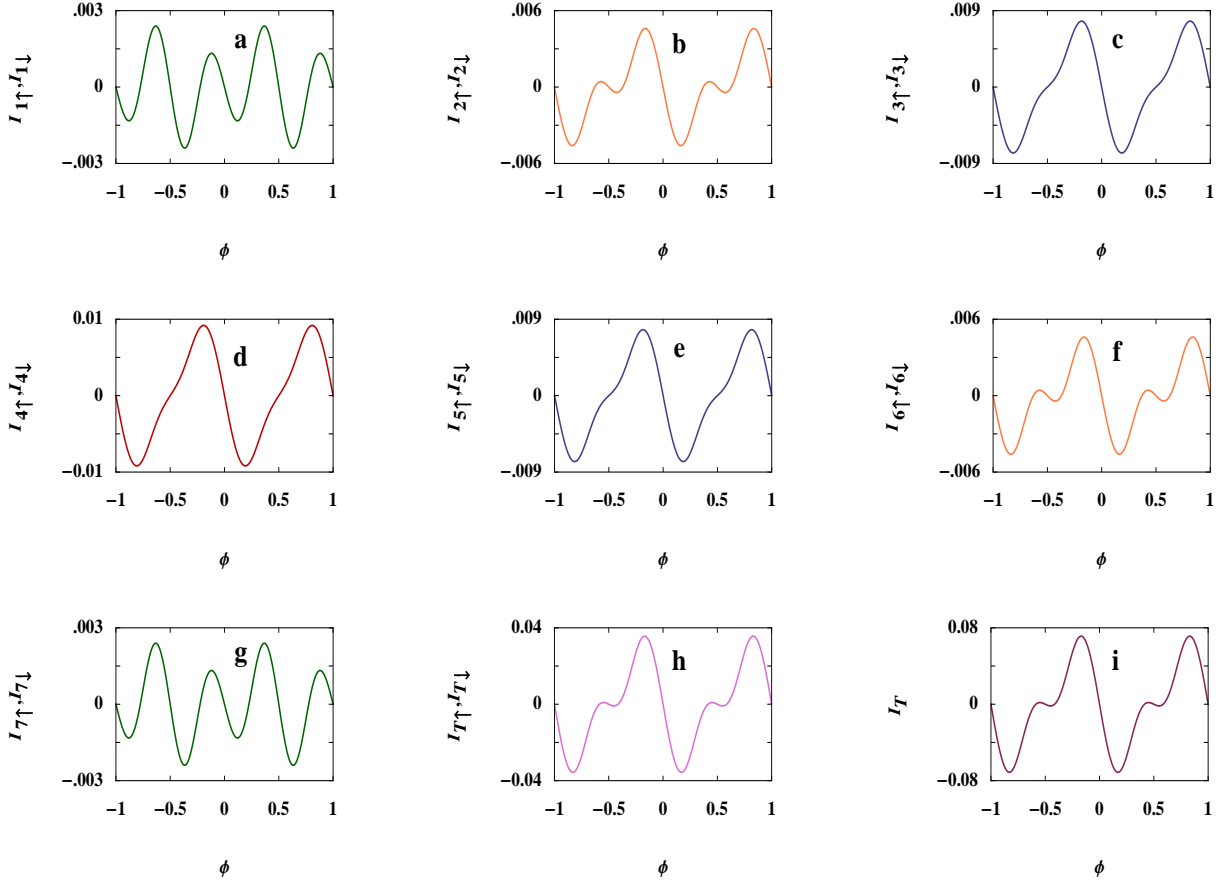


FIG. 12: (Color online). Persistent current in individual zigzag paths as a function of ϕ for a half-filled zigzag nanotube ($N_x = 20$ and $N_y = 7$) with $U = 1.2$, where, (a)-(g) correspond to 1st-7th zigzag channels of the tube, respectively. The net current corresponding to both up and down spin electrons are displayed in (h) while in (i) total persistent current is shown.

and 1.5, respectively. The energy levels evince one flux-quantum periodicity, as expected, and their energies get increase with U . It can be explained as follows. In presence of U , each site is occupied by an electron with either up or down spin in the half-filled band case. This is the ground state energy configuration. Now, if we add an electron further, the probability of getting two opposite spin electron in a single site becomes finite which gives higher energy due to the repulsion in presence of U .

VI. CURRENT-FLUX CHARACTERISTICS

Now we focus our attention on the behavior of persistent current in a zigzag nanotube.

First, we illustrate the dependence of persistent current amplitude on the electron filling. To ensure it in Fig. 11 we present the current-flux characteristics of a zigzag nanotube considering $N_x = 14$ and $N_y = 6$, where four different figures correspond to the four different cases of electron filling. The Hubbard interaction strength is set at 1. It is observed that when the number of electrons is much smaller than half-filling, persistent cur-

rent exhibits multiple kinks at different values of ϕ , associated with the multiple crossings of energy levels, as shown in Figs. 11(a)-(c). In these three cases the num-

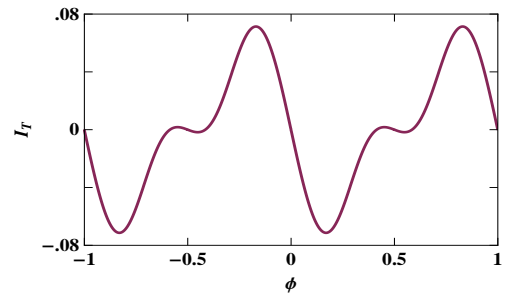


FIG. 13: (Color online). Total persistent current obtained in a traditional derivative approach (Eq. 19) as a function of ϕ for the same parameter values mentioned in Fig. 12.

ber of electrons are 10, 20 and 30, respectively. This is quite analogous to the nature of persistent current observed in conventional multi-channel mesoscopic cylinders. The behavior of persistent current gets significantly

modified when the nanotube becomes half-filled or nearly half-filled. For example, see Fig. 11(d). Here we choose $N_e = 82$ i.e., the nanotube is very near to the half-filled band case. In such a case all the kinks disappear and current varies almost continuously, analogous to the behavior of persistent current observed in traditional single-channel mesoscopic rings. For the cases when the nanotube is far away from half-filling, current amplitudes are quite comparable to each other (see Figs. 11(a)-(c)). On the other hand, when the tube is nearly half-filled current amplitude remarkably gets suppressed. It is illustrated

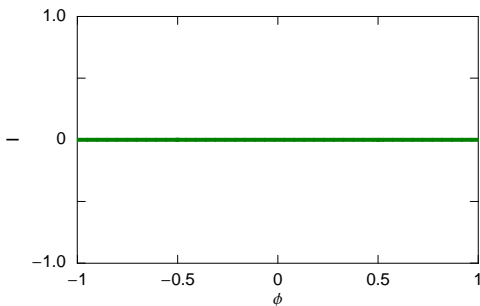


FIG. 14: (Color online). Persistent current in an armchair path as a function of ϕ for a zigzag nanotube with the same parameter values as mentioned in Fig. 12.

in Fig. 11(d). This enormous reduction of current amplitude can be visualized from the E - ϕ characteristics given in Fig. 7. At half-filling or very close to half-filling, the top most filled energy level lies in the nearly flat region i.e., around $E = 0$ (see Fig. 7(a)) and it contributes a little to the current. Moreover, when $U \neq 0$, there is gap in the midband region. Now, for a particular filling the net persistent current is obtained by taking the sum of individual contributions from the lowest filled energy levels, and, in this process only the contribution which comes from the highest occupied energy level survives finally and the rest disappear due to their mutual cancellations. It leads to the enormous reduction of persistent current amplitude in the half-filled or nearly half-filled case. This feature is independent of the size of the nanotube. In all these cases, persistent current varies periodically with flux ϕ , exhibiting ϕ_0 flux-quantum periodicity. From these current-flux spectra we can emphasize that, the current amplitude in a zigzag nanotube is highly sensitive to the electron filling and this phenomenon can be utilized *in designing a high conducting to a low conducting switching operation and vice versa*.

Finally, we concentrate on the behavior of persistent current in separate branches of a zigzag carbon nanotube. As illustrative examples, in Fig. 12 we show the variation of persistent current in individual zigzag paths as a function of flux ϕ for the half-filled case considering $N_x = 20$ and $N_y = 7$, where (a)-(g) correspond to 1st-7th zigzag channels of the tube, respectively. The Hubbard correlation strength U is set equal to 1.2. In each of these figures we display currents carried by both up and down spin

electrons together. They are exactly superposed with each other. All these currents exhibit ϕ_0 flux-quantum periodicity and their magnitudes are quite comparable to each other. Interestingly we see that $I_{1\uparrow}$ is exactly identical to $I_{7\uparrow}$, and, similarly for the $(I_{2\uparrow}, I_{6\uparrow})$ and $(I_{3\uparrow}, I_{5\uparrow})$ pairs. $I_{4,\uparrow}$, the current in the middle channel, becomes the isolated one since we have chosen $N_y = 7$. This is true for any zigzag nanotube with odd N_y . For a tube with even N_y , currents are pairwise identical. Summing up the individual currents in seven zigzag channels we get net persistent current carried by up and down spin electrons in the nanotube which is presented in Fig. 12(h) and the total current is displayed in Fig. 12(i) which exactly matches with the total current derived from the conventional method where first order derivative of the ground state energy is taken into account, as shown in Fig. 13. It emphasizes that the net contribution of persistent current in a zigzag carbon nanotube comes only from the individual zigzag channels, not from the armchair paths. To justify it in Fig. 14 we present the variation of persistent current in an armchair path as a function of ϕ for a half-filled zigzag nanotube considering $N_x = 20$ and $N_y = 7$, which clearly shows zero current for the entire range of ϕ .

VII. SUMMARY

To conclude, in the present work we investigate in detail the magnetic response of a zigzag nanotube, threaded by a magnetic flux ϕ , using a generalized Hartree-Fock mean field approach. The model is described by a simple tight-binding framework. Following the E - k_x spectra of both the non-interacting and interacting cases of a finite width nanoribbon, we present the results of a nanotube with zigzag edges. Energy levels get modified significantly in the presence of Hubbard interaction and the nature of the energy spectrum strongly depends on the electron filling. At the half-filled bad case, a gap opens up at the Fermi energy which is consistent with the DFT calculations. Next, we establish the second quantized form to evaluate persistent current in individual paths of a zigzag carbon nanotube. From the current-flux characteristics we can emphasize that the current amplitude in the zigzag nanotube is highly sensitive to the electron filling and this phenomenon can be utilized in designing a high conducting to a low conducting switching device and vice versa.

ACKNOWLEDGMENTS

First author (PD) thanks M. Dey and N. S. Das for their help in drawing the colored figures of the nanoribbon and tube.

-
- [1] A. K. Geim and K. S. Novoselov, *Nat. Mater.* **6**, 183 (2007).
- [2] A. H. Castro Neto, F. Guinea, N. M. R. Peres, K. S. Novoselov, and A. K. Geim, *Rev. Mod. Phys.* **81**, 109 (2009).
- [3] K. S. Novoselov, A. K. Geim, S. V. Morozov, D. Jiang, M. I. Katsnelson, I. V. Gorieva, S. V. Dubonos, and A. A. Firsov, *Nature* **438**, 197 (2007).
- [4] O. O. Kit, T. Talliner, L. Mahadevan, J. Timonen, and P. Koskinen, arXiv:1108.0048v1.
- [5] S. K. Maiti, *Solid State Commun.* **150**, 2212 (2010).
- [6] S. K. Maiti, *Phys. Status Solidi B* **248**, 1933 (2011).
- [7] S. K. Maiti and A. Chakrabarti, *Phys. Rev. B* **82**, 184201 (2010).
- [8] M. Büttiker, Y. Imry, and R. Landauer, *Phys. Lett.* **96A**, 365 (1983).
- [9] B. L. Altshuler, Y. Gefen, and Y. Imry, *Phys. Rev. Lett.* **66**, 88 (1991).
- [10] A. Schmid, *Phys. Rev. Lett.* **66**, 80 (1991).
- [11] V. Ambegaokar and U. Eckern, *Phys. Rev. Lett.* **65**, 381 (1990).
- [12] L. P. Levy, G. Dolan, J. Dunsmuir, and H. Bouchiat, *Phys. Rev. Lett.* **64**, 2074 (1990).
- [13] V. Chandrasekhar, R. A. Webb, M. J. Brady, M. B. Ketchen, W. J. Gallagher, and A. Kleinsasser, *Phys. Rev. Lett.* **67**, 3578 (1991).
- [14] E. M. Q. Jariwala, P. Mohanty, M. B. Ketchen, and R. A. Webb, *Phys. Rev. Lett.* **86**, 1594 (2001).
- [15] R. Deblock, R. Bel, B. Reulet, H. Bouchiat, and D. Mailly, *Phys. Rev. Lett.* **89**, 206803 (2002).
- [16] K. Sasaki, S. Murakami, R. Saito, and Y. Kawazoe, *Phys. Rev. B* **71**, 195401 (2005).
- [17] R. B. Chen, B. J. Lu, C. C. Tsai, C. P. Chang, F. L. Shyu, and M. F. Lin, *Carbon* **42**, 2873 (2004).
- [18] M. Szopa, M. Marganska, and E. Zipper, *Phys. Lett. A* **299**, 593 (2002).
- [19] H. F. Cheung, Y. Gefen, E. K. Riedel, and W. H. Shih, *Phys. Rev. B* **37**, 6050 (1988).
- [20] S. K. Maiti, *Physica E* **31**, 117 (2006).
- [21] S. K. Maiti, *Solid State Phenom.* **155**, 87 (2009).
- [22] S. Bellucci and P. Onorato, *Physica E* **41**, 1393 (2009).
- [23] P. A. Orellana and M. Pacheco, *Phys. Rev. B* **71**, 235330 (2005).
- [24] L. K. Castelano, G. -Q. Hai, B. Partoens, and F. M. Peeters, *Phys. Rev. B* **78**, 195315 (2008).
- [25] M. P. López Sancho, M. C. Muñoz, and L. Chico, *Phys. Rev. B* **63**, 165419 (2001).
- [26] H. Lin, J. Lagoute, V. Repain, C. Chacon, Y. Girard, J. -S. Lauret, F. Ducastelle, A. Looiseau, and S. Rousset, *Nature Mater.* **9**, 235 (2010).
- [27] S. Sorella and E. Tosatti, *Europhys. Lett.* **19**, 699 (1992).
- [28] R. Heyd, A. Charlier, and E. McRae, *Phys. Rev. B* **55**, 6820 (1997).
- [29] K. Wakabayashi, M. Fujita, H. Ajiki, and M. Sigrist, *Phys. Rev. B* **59**, 8271 (1999).
- [30] L. Brey and H. A. Fertig, *Phys. Rev. B* **73**, 235411 (2006).
- [31] K. Wakabayashi and K. Harigaya, *J. Phys. Soc. Jpn.* **72**, 998 (2003).
- [32] J. Fernández-Rossier, *Phys. Rev. B* **77**, 075430 (2008).
- [33] Y. Son, M. L. Cohen, and S. G. Louie, *Nature (London)* **444**, 347 (2006).
- [34] S. K. Maiti, S. Saha, and S. N. Karmakar, *Eur. Phys. J. B* **79**, 209 (2011).
- [35] S. K. Maiti, *J. Appl. Phys.* **110**, 064306 (2011).